Journal of Power Sources 240 (2013) 1–7

Contents lists available at SciVerse ScienceDirect

Journal of Power Sources

journal homepage: www.elsevier.com/locate/jpowsour

Micro fuel cell utilizing fuel cell water recovery and pneumatic valve

S. Eickhoff [a,b,*], C. Zhang [b], T. Cui [a]

[a] Department of Mechanical Engineering, University of Minnesota, 111 Church Street SE, Minneapolis, MN 55455, USA
[b] Honeywell International, Automation and Control Solutions Research Laboratory, Plymouth, MN 55441, USA

HIGHLIGHTS

- MFC utilizes vapor hydrolysis, water recovery, and a pneumatic valve.
- Integrated MFCs were developed and tested, and achieved 987 Wh L^{-1}.
- Energy density greater than 2000 Wh L^{-1} should be possible in optimized MFCs.

ARTICLE INFO

Article history:
Received 5 November 2012
Received in revised form
24 March 2013
Accepted 25 March 2013
Available online 9 April 2013

Keywords:
Micro fuel cell
Self regulation
Passive pneumatic valve
Chemical hydride
Water recovery

ABSTRACT

Micro fuel cells (MFCs) defined by an average power output of less than 10 W offer the potential to improve the runtime and performance of portable devices by providing significantly higher energy density (energy per unit volume) than batteries. However, despite several decades of intense research and development, MFCs have yet to realize this potential, and no MFC technology has achieved broad market adoption. We report in this article an MFC which utilizes water-vapor-driven hydride hydrolysis, fuel cell water recovery, and a self-regulating pneumatic valve to achieve higher energy density than conventional batteries. Integrated MFC prototypes were developed and tested, and achieved 987 Wh L^{-1}. Further improvements in energy density are possible by optimizing the fuel pellet configuration (density, geometry, particle size and distribution, etc.). Energy density greater than 2000 Wh L^{-1} may be possible in optimized MFCs discharged at low power.

1. Introduction

The design of portable electronic devices reflects a compromise among a range of competing interests including size, performance, and battery lifetime. While the performance of portable devices as defined by disk space, CPU speed, and available RAM continues to advance at an exponential rate approximating Moore's Law, battery performance as defined by energy density (energy per unit volume) is increasing linearly (Fig. 1), creating an ever-widening gap between the potential and actual performance of portable devices [1]. Micro fuel cells (MFCs) (defined here as fuel cells producing <10 W average power) offer the potential to bridge this gap by providing a 5–10× increase in energy density vs. batteries. However, despite several decades of intense research and development, MFCs have yet to realize this potential, and no MFC technology has achieved broad market adoption.

Although many MFC approaches have been attempted as described elsewhere [2], among the most promising are those that store hydrogen in chemical hydrides, release the hydrogen via water vapor hydrolysis, and convert the hydrogen to electrical energy in a hydrogen–air proton exchange membrane (PEM) fuel cell. This approach is considered favorable because chemical hydrides have inherently high energy density, water vapor–hydrolysis reactions are relatively easy to regulate and have high yield, and PEM fuel cells are simple to construct, amenable to scaling, and capable of high chemical-to-electrical conversion efficiency.

The advantages of using water vapor (instead of liquid water) to carry out the hydrolysis reaction are well documented. Kong et al. carried out hydrolysis reactions with several commercially available hydrides (CaH_2, LiH, $LiAlH_4$, $NaAlH_4$) using both liquid water and water vapor, and found that the hydrolysis reactions were more controllable and generally had higher reaction yield when carried out with water vapor [3].

* Corresponding author. Department of Mechanical Engineering, University of Minnesota, 111 Church Street SE, Minneapolis, MN 55455, USA. Tel.: +1 763 954 2380; fax: +1 763 954 2504.
E-mail addresses: steven.eickhoff@honeywell.com, steveneickhoff@yahoo.com (S. Eickhoff).

0378-7753/$ – see front matter © 2013 Elsevier B.V. All rights reserved.
http://dx.doi.org/10.1016/j.jpowsour.2013.03.152

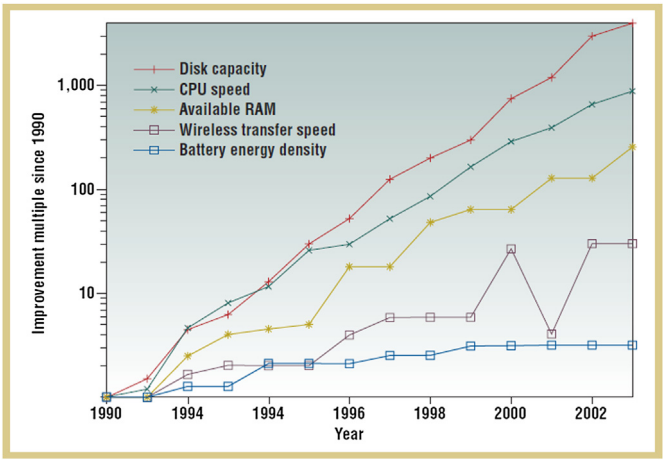

Fig. 1. Improvements in portable electronic device components from 1990 to 2003 [1].

Several MFCs using hydride hydrolysis with water vapor have been reported in the literature. Wood et al. reported an Electrical Power Generator using a water vapor generator comprised of a liquid water reservoir and vapor-permeable liquid-impermeable membrane, coupled to a hydride bed to generate hydrogen, and a miniature PEM fuel cell [4]. This Electrical Power Generator utilizes a micro controller, sensors, and an electrically controlled valve to regulate the power output of the system by controlling water vapor transport from the water vapor generator to a hydride bed. No experimental data or performance projections were provided, however the complexity of the balance of plant (sensors, valve, micro controller) would likely limit energy density. Rezachek et al. report an MFC with a passive pneumatic valve to regulate water vapor transport from a liquid water source to a hydride fuel, based on the pressure difference across a diaphragm [5]. This approach is an improvement over Wood et al. in that it eliminates much of the BOP, which should improve system energy density. Moghaddam et al. report a similar passive regulation scheme, however it differs from Rezachek et al. in that they utilized a membrane that deflects based on the pressure difference across a diaphragm, which blocks a water port and stops hydrogen generation [6,7]. Each of the MFCs described above have an on-board liquid water reservoir which generates the water vapor used in the hydrolysis reaction, and these reservoirs typically occupy >50% of the total volume of the MFC. If a means could be found to eliminate the water reservoir, the energy density of these MFCs could more than double.

This author first demonstrated an MFC without a water reservoir, replacing it with water vapor recovered from the fuel cell [8]. Water vapor generated at the fuel cell cathode permeates the PEM from cathode to anode, driven by a water vapor concentration gradient in the PEM, with is created by closely positioning the hygroscopic hydride to the fuel cell anode. MFCs utilizing water vapor recovery were built, and very high energy densities (>2000 Wh L^{-1}) were demonstrated [9]. Water vapor recovery using this method was subsequently reported by Zhu et al., although their reported energy density was much lower (313 Wh L^{-1}) due in part to the large fraction of the device volume that was occupied by packaging [10].

The power output of MFCs using water recovery is highly sensitive to ambient humidity as described by Zhu et al., due to the inherent requirement that the humidity at the fuel cell's cathode remains in equilibrium with the ambient environment. This humidity sensitivity, coupled with the unregulated nature of early MFCs using water vapor recovery, makes them unsuitable for portable devices in their current form. A means of regulating these water-recycling MFCs is required to make them practical for portable devices.

This paper describes an MFC utilizing water recovery and a pneumatic valve to regulate the hydrogen generation rate. It includes a detailed discussion of the MFC design, fabrication process, and testing methodology, as well as performance data for the MFC components and integrated device.

2. Experimental

The MFC (Fig. 2) is 14 mm in diameter and 50 mm in height, and has a total volume of 7.7 cc. The MFC has a nominal operating potential of 1.5 V, however because it uses two hydrogen–air PEM fuel cells in a series electrical configuration, the open circuit potential is ~1.9 V. The two circumferentially perforated bands in the metal case provide air access to the fuel cells. The cylindrical portion of the metal case acts as the MFC's cathode electrode, while the circular metal plate at the bottom acts as the anode.

2.1. Operating principle

The MFC shown schematically in Fig. 3 is comprised of a hydrogen–air PEM fuel cell coupled to a self regulating hydrogen generator. Hydrogen produced by the hydrogen generator and oxygen from ambient air react at the fuel cell, generating electrical energy, water vapor, and waste heat (not shown) by the following reactions:

$$\text{Fuel cell anode reaction}: \quad 4H_2 \rightarrow 8H^+ + 8e^-$$

$$\text{Fuel cell cathode reaction}: \quad 2O_2 + 8H^+ + 8e^- \rightarrow 4H_2O$$

$$\text{Overall reaction}: \quad 4H_2 + 2O_2 \rightarrow 4H_2O + \text{Energy} \qquad (1)$$

Water vapor generated at the fuel cell cathode back-diffuses through the PEM and reacts with the chemical hydride to generate hydrogen by the following reaction:

$$LiAlH_4 + 4H_2O \rightarrow 4H_2 + \text{Solids} \qquad (2)$$

Fig. 2. Photograph of an MFC next to quarter for reference.

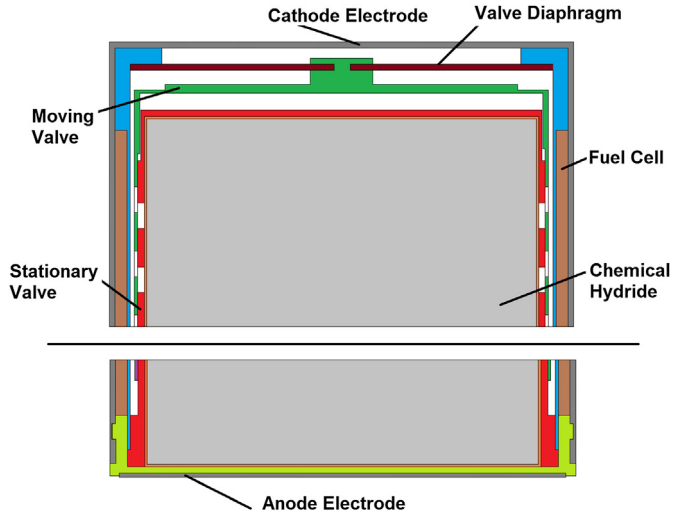

Fig. 3. Cross section schematic of the MFC. The middle portion of the MFC is removed to more clearly show the top and bottom.

Summing reactions (1) and (2) gives the overall reaction (3) of the MFC as:

$$LiAlH_4 + 2O_2 \rightarrow Energy + Solids \quad (3)$$

The overall reaction is water neutral, generates no gas phase byproducts, and consumes only oxygen from the air.

The hydrogen generation rate is regulated by a passive, pneumatic diaphragm valve which controls diffusive transport of water vapor from the fuel cells to the chemical hydride, based on the pressure difference (ambient minus internal) across the diaphragm. When an electrical load is placed on the MFC, hydrogen is consumed by the fuel cell, causing the internal pressure to drop and the diaphragm to deflect inward. This opens the valve, and allows water vapor to diffuse to and react with the fuel, generating hydrogen. When the load is removed, the pressure inside the MFC rises, causing the diaphragm to deflect outward which closes the valve and stops hydrogen generation. The valve is partially open during normal operation, and only closes or opens completely under no-load or maximum-load conditions, respectively.

Fig. 4 shows a photograph of the MFC components. The detailed design and function of the MFC components will be described in the following sections.

2.2. Fuel cell

The planar fuel cell (Fig. 5) is comprised of 5 layers "stacked" up and compressed together, forming a monolithic and flexible stack which is wrapped around the anode support. The fuel cell consists of an anode electrode, anode adhesive layer with embedded anode gas diffusion layers, MEA in polyimide frame, cathode adhesive layer with embedded cathode gas diffusion layers, and cathode electrode.

The anode and cathode current collectors are formed by patterning (with a shadow mask) an evaporated metal film (50 Å Ti, 1 μ Au) on a PET substrate (Fralock, Valencia, CA), (25 μ thick). The Ti functions as an adhesion layer between the Au and the PET

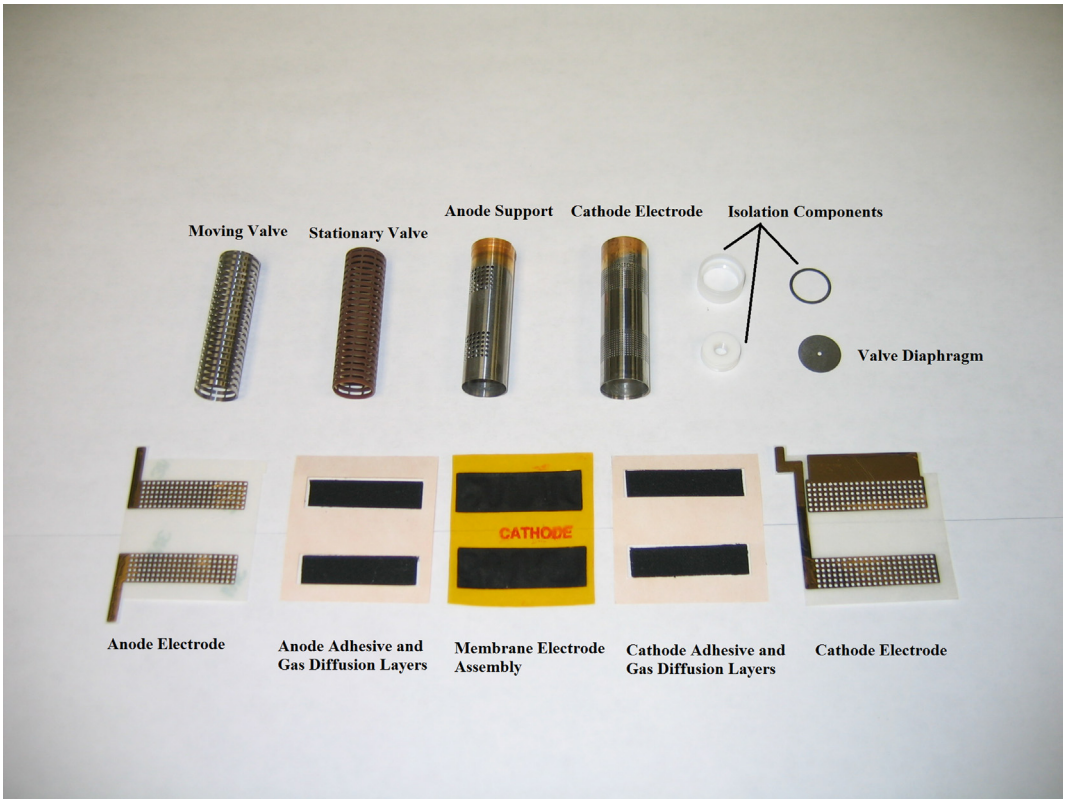

Fig. 4. Photograph of MFC components. The fuel cell stack components occupy the bottom row, and include (from left to right) an anode electrode, anode adhesive layer with embedded anode gas diffusion layers (two black rectangles), MEA in polyimide frame (black rectangles in orange film), cathode adhesive layer with embedded cathode gas diffusion layers, and cathode electrode. The mechanical components occupy the top row, and include (from left to right) moving valve, stationary valve, anode support (for the FC stack), the cathode electrode, electrical isolation components, and the valve diaphragm. (For interpretation of the references to color in this figure legend, the reader is referred to the web version of this article.)

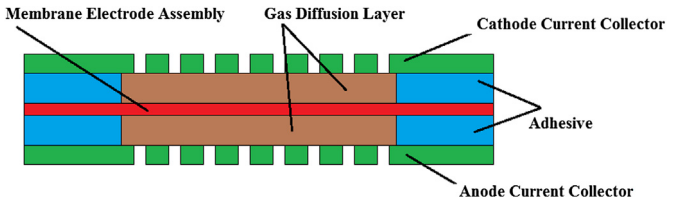

Fig. 5. Cross section schematic of the planar fuel cell.

substrate. The current collector perimeter and holes are cut with a laser (Universal Laser Systems, Scottsdale, AZ). The anode and cathode adhesive layers are three layer stacks comprises a 25 μ thick polyimide layer sandwiched between 25 μ adhesive layers (Fralock, Valencia, CA). The cathode and anode gas diffusion layers are 100 μ thick carbon paper (Ballard, Burnaby, BC) cut to fit the "window" in the adhesive layers. The MEA in polyimide frame comprises a catalyst electrode-coated 25 μ thick Nafion membrane embedded in a 25 μ thick polyimide frame (Ion Power, New Castle, DE). The MEA has an active area of 3 cm^2 per cell, or 6 cm^2 total for the two cells.

The fuel cell is assembled by stacking the layers on top of one another sequentially (from left to right, in Fig. 4) and compressing them together with one metric ton of force using a hydraulic press (Carver, Wabash, IN). The fuel cell is then wrapped around and adhered to the anode support.

2.3. Diaphragm valve

The diaphragm valve comprises a flexible diaphragm, a moving valve, and a stationary valve. The moving valve is connected to center of the flexible diaphragm, coupling the movements in the flexible diaphragm (caused by changes in the differential pressure across the diaphragm) to the moving valve. The moving and stationary valves have identical perforation patterns (slots) that are aligned when the valve is completely open (diaphragm fully deflected inwards), and misaligned when the valve is completely shut (diaphragm fully deflected outwards). The degree of alignment of the moving and stationary valves determines the conductance of the valve, and therefore the hydrogen generation rate. The moving and stationary valves in open and closed position are shown schematically in Fig. 6.

The diaphragm is cut from 25 μ thick PET film (Fralock, Valencia, CA) with a laser (Universal Laser Systems, Scottsdale, AZ). The moving valve is CNC machined from brass tubing, while the stationary valve is CNC machined from 316 stainless steel tubing. A low viscosity oil lubricant (BP Lubricants, Baltimore MD) film is applied between the fixed and moveable valves to reduce friction and to improve sealing.

2.4. Chemical hydride fuel

The chemical hydride fuel is comprised of LAH powder (Sigma Aldrich, St. Louis, MO) compressed into pellets, without a binder or filler. The powder is used as-received from the manufacturer, and has the particle size distribution as shown in Fig. 7. The particle size distribution was determined by separating the raw powder using sieves (Dual Manufacturing, Chicago IL) with progressively smaller mesh sizes (160 μm, 125 μm, 90 μm 63 μm 45 μm, 32 μm, 20 μm).

The powder is compressed in stages inside the stationary valve using a hydraulic press (Carver, Wabash, IN). Pellets of varying density were tested, typically ranging from ~0.4 to 0.8 g cc^{-1}. Although particle size and distribution is expected to impact system performance, it is beyond the scope of this work, and will be explored in a subsequent paper.

2.5. Mechanical components

The mechanical components (Fig. 8) comprise the anode and cathode (output) electrodes and the anode support. The mechanical components are CNC-machined from 316 stainless steel tubing. The anode support provides mechanical support for the fuel cell stack. The anode (output) electrode is connected to the anode of the fuel cell stack, and provides the electrical and mechanical interface to the load. The cathode (output) electrode compresses the fuel cell stack against the anode support; it is connected to the cathode of the fuel cell stack, and provides the electrical and mechanical interface to the load.

3. Results and discussion

In the following section the performance of the fuel cell stack and valve will first be presented, followed by the system-level performance under constant current and constant potential discharge. The valve is tested prior to insertion of the fuel, while

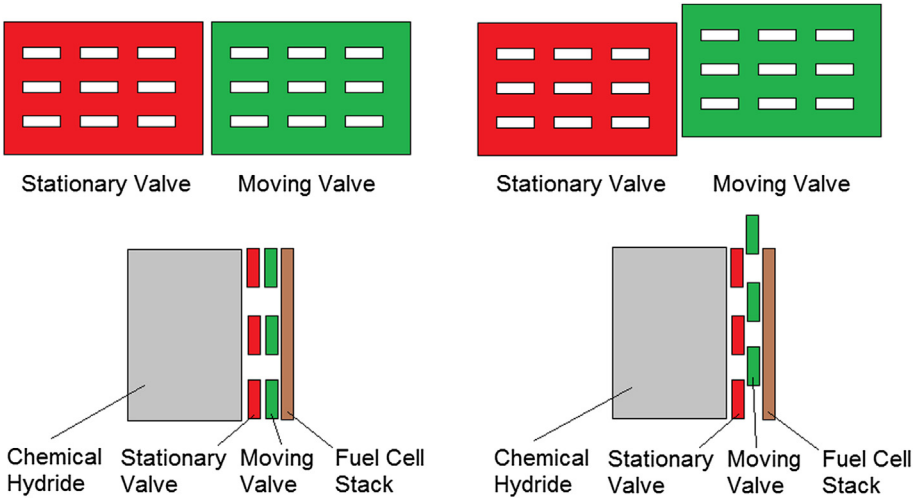

Fig. 6. Schematic of valve in open (left) and closed (right) positions. The position of the moving valve controls the conductance path between the fuel cell stack and the chemical hydride.

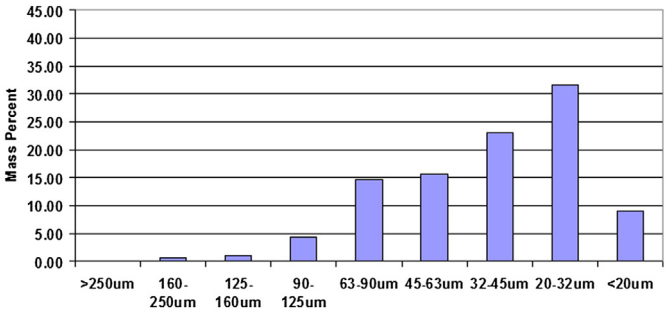

Fig. 7. LAH particle size distribution.

the fuel cell stack is tested both before and after insertion of the fuel.

3.1. Fuel cell stack

Fuel cell stacks were tested with a potentiostat (Maccor, Tulsa, OK). Current and potential were recorded as the cell potential was stepped in 0.1 V increments from open circuit to 0.8 V. Bottled dry hydrogen gas (Toll Gas, Plymouth, MN) at 1 atm pressure flowing at 100 sccm was fed to the interior of the MFC; excess flow was exhausted to ambient. Tests were conducted in a "dead-end" configuration to simulate performance under real operating conditions (i.e. no bulk flow past the anode); thus the anode stoichiometry was one even though excess hydrogen flow was exhausted to ambient. Tests were performed in a temperature and humidity controlled environment at 20 °C, 50% relative humidity, using an oven (Thermotron, Holland MI) and a bubbler system.

A polarization curve for the MFC running on bottled hydrogen gas is shown in Fig. 9. The open circuit potential is 1.9 V, with a peak power of 575 mW (95.8 mW cm^{-2}) occurring at 0.8 V. By comparison, Kim et al. demonstrated a peak power density of 128 mW $cm^{-2}$with a similarly configured planar air breathing fuel cell [11]. The higher peak power density they reported is likely attributable in part to the use of humidified hydrogen. The MFC exhibits the typical decrease in potential with increasing current due to activation, ohmic, and concentration polarization.

A polarization curve for the MFC running on LAH is shown in Fig. 10. The open circuit voltage (1.9 V) is similar to the test performed with bottled hydrogen gas, however the peak power is lower (160 mW, 26.7 mW cm^{-2}), and slope of the voltage vs. current curve is larger, indicating higher internal resistance. This is expected for two reasons: First, the highly hygroscopic LAH is positioned closely to the fuel cell anode to enable fuel cell water recovery. This dries the PEM somewhat and reduces its ionic conductivity (which is strongly depended on hydration), resulting in

Fig. 8. Mechanical components including the anode support (left), cathode electrode (center) and the anode electrode (right). The top of the anode support and cathode electrode are electroplated with gold to reduce contact resistance.

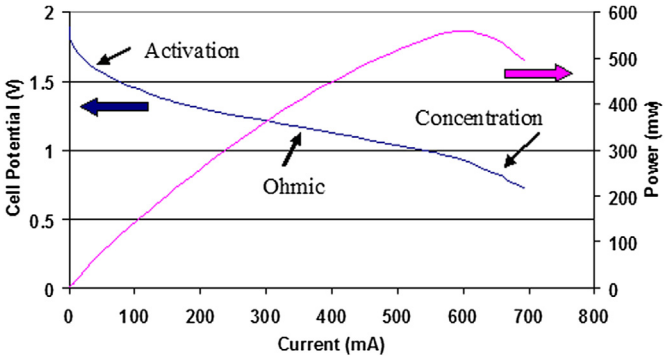

Fig. 9. Polarization curve with bottled hydrogen gas in a dead-end configuration (anode stoichiometry of one). The MFC exhibits the typical decrease in potential with increasing current due to activation, ohmic, concentration polarization.

higher internal resistance. Second, electroosmotic drag (in which water molecules are dragged from anode to cathode by migrating protons) places an upper limit on current density, because the water back-diffusion rate in the PEM and consumption rate by the LAH fuel must be balanced to sustain power output in water recycling fuel cells.

Activation and Ohmic contributions to polarization are clearly visible in Fig. 9, however the increasingly negative slope at high current which indicates concentration polarization, is largely absent. This occurs because the maximum current density in water recycling MFCs is typically limited by the hydrogen generation rate, not oxygen transport to the cathode or hydrogen transport to the anode, as in conventional fuel cells operating at high current. Once the hydrogen generation limit is reached in a water recycling MFC, further increases in the load serve only to reduce the cell potential.

The data presented in Fig. 10 were taken at the beginning of the discharge of a fresh MFC, and changes throughout discharge. The long-term performance of the MFC under constant current and constant potential discharge tests shows these changes, and is presented below.

3.2. Diaphragm valve

The performance of the valve is characterized by measuring the movement of the diaphragm with a laser micrometer (Keyence, Itasca, IL) as the absolute pressure inside the MFC is varied between 8 and 18 psig. The valve is designed to fully open at <8 psig and fully close at >18 psig, and achieve a total travel of 600 μm. The numerical value of the starting and end points are arbitrary and determined by the initial distance between the valve diaphragm

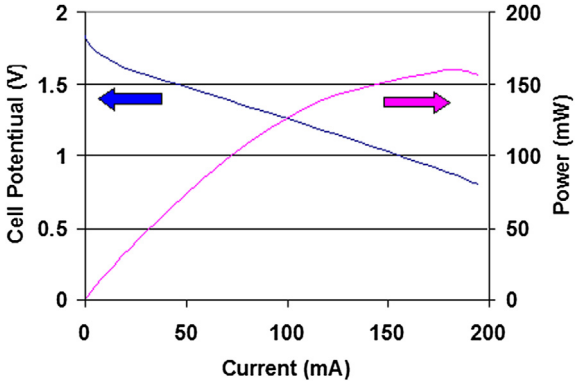

Fig. 10. Polarization data for MFC with LAH fuel.

and the laser micrometer. Total travel is limited to 600 μm by stops built into the valve. A typical valve performance curve for the MFC is shown in Fig. 11. The pressure inside the MFC is cycled between 8 and 18 psig; the valve diaphragm responds to the pressure change by moving from its fully closed position (at −420 μm) to its fully open position (at 160 μm), and achieves a total travel of 580 μm, which is suitably close to the design value for the MFC to function properly. Hysteresis is attributed to the friction between the fixed and moveable valves.

3.3. MFC system performance

MFC performance was characterized with a potentiostat running constant current and constant potential discharge tests in a temperature and humidity controlled ambient air environment held at 20 °C and 50% relative humidity. Current and potential were monitored as a function of time until the MFC could no longer sustain the desired current or potential. Delivered energy and system energy density were calculated based on the potential and current data.

The system-level tests were performed after the valve and fuel cell component tests described earlier. Following the component-level testing, the MFCs underwent a fueling and flushing process comprised of packing the desired amount of fuel in the fuel chamber (described above), then flushing the fuel chamber for 5 min each with nitrogen gas and hydrogen gas at a flow rate of 100 sccm. The MFCs were then sealed with a fast-curing epoxy and placed under test.

A typical constant current discharge curve for the MFC is shown in Fig. 12. The test was conducted at 20 mA constant current with 1.75 g of LAH fuel. 20 mA was chosen because it reflects the typical current consumption of low-rate applications for portable devices.

The initial cell potential was 1.5 V, and slowly decayed to 1.35 V after 35 h, where it remains until about 110 h, when it suddenly dropped to about 1.3 V, before recovering slowly to 1.35 V. At 150 h the potential dropped quickly from 1.35 V to the 1 V cutoff, marking the end of the test, and indicating that the MFC can no longer sustain 20 mA.

We hypothesize that the potential decay from 1.5 V to 1.35 V during the first 35 h of the test is likely due to atmospheric nitrogen permeating the PEM and reducing the partial pressure of hydrogen in the MFC. Changes in anode humidification levels are another possible explanation for the potential decay, however since the anode humidity is expected to rise over time due to increasing diffusion resistance in the fuel reaction products, this effect would be expected to increase, not decrease the cell potential.

The cause of the potential reduction from 1.35 V to 1.3 V which occurred at ∼110 h is unknown, however we hypothesize that the valve may have become stuck, causing a temporary reduction in system pressure and cell potential before recovering when the valve again became free. Hysteresis in the valve deflection curve (Fig. 11) suggests that substantial friction occurs during valve movement. We expect to confirm this hypothesis in future tests by monitoring the internal pressure and real-time position of the valve throughout the test.

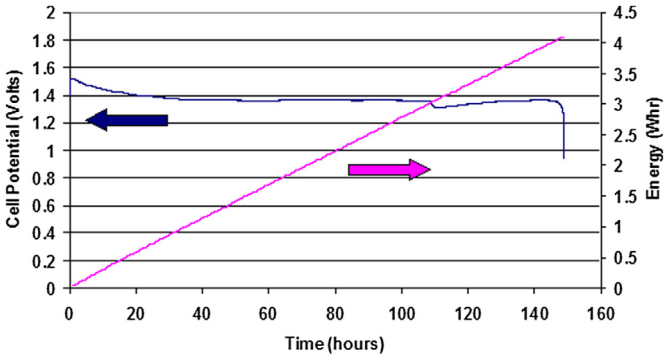

Fig. 12. 20 mA constant current discharge.

The total energy extracted from the 7.7 cc MFC was 4.1 Wh, which corresponds to a system energy density of 532 Wh L^{-1}. The projected energy in the 1.75 g of LAH fuel (converted by the fuel cell at the average potential during the test) is 6.7 Wh, thus the 4.1 Wh of delivered energy corresponds to an LAH reaction yield of 61%. The low reaction yield indicates an incomplete hydride–water reaction, and/or a hydrogen leak in the system. A test at 10 mA constant current performed immediately after the 20 mA test extracted an additional 1.3 Wh, confirming an incomplete reaction. An examination of the fuel reaction products after the 10 mA test indicated that some un-reacted fuel remained, though the amount is unknown.

In order to extract all of the energy in the fuel and to better understand the maximum power output vs. time, constant potential tests were also performed on the MFC. Fig. 13 shows the results of a typical constant potential test. The cell potential was held at 1.2 V with a potentiostat and the current was recorded as a function of time.

The initial power decayed quickly from 110 mW to 90 mW (18.3 mW cm^{-2} to 15.0 mW cm^{-2}), after which it decayed more slowly, ultimately reaching zero at ∼480 h. The total extracted energy was 7.6 Wh from 2.4 g of LAH fuel, corresponding to an energy density of 987 Wh L^{-1}, and a reaction yield of 90%.

We hypothesize that the initial power decay occurs as the outer surface of the fuel pellet reacts and forms a product layer which

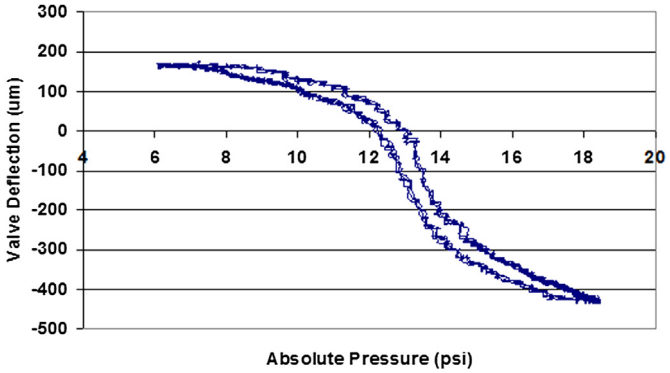

Fig. 11. Valve deflection vs. absolute pressure, as the pressure in the MFC is cycled from 8 to 18 psi.

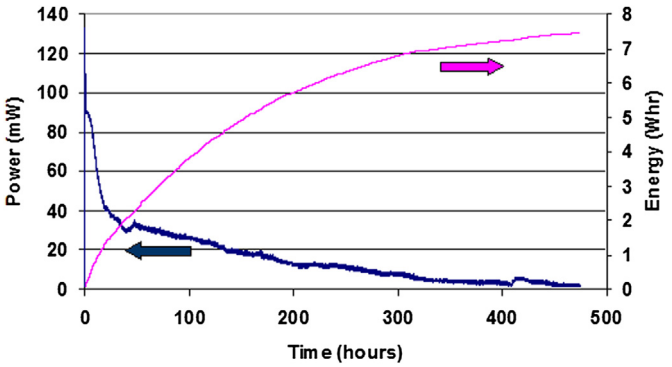

Fig. 13. Constant potential (1.2 V) discharge.

rapidly increases the diffusion resistance at the surface and slows the hydrogen generation rate.

The long-term decay is thought to be caused by an exponentially-increasing diffusion resistance that occurs as the reaction front moves radially through the pellet, as both the physical distance the water vapor travels and the pellet density increase. The effects of increasing diffusion resistance over time are not readily apparent in constant current discharge tests (until the end of the test) because the valve controls the hydrogen generation rate to maintain constant pressure. The test ends when the consumption rate can no longer be met by the hydrogen generation rate due to rising diffusion resistance in the fuel. Optimizing this decay to improve energy density and power output will require a deeper understanding of the parameters that impact diffusion resistance, including initial pellet density, pellet geometry, particle size and distribution, potential side reactions, and others. This optimization is beyond the scope of this work, but will be explored in a subsequent paper.

4. Conclusion

We report in this article an MFC which utilizes water-vapor-driven hydride hydrolysis, fuel cell water recovery, and a self-regulating pneumatic valve to achieve higher energy density than conventional batteries. Integrated MFCs were developed and tested, and achieved 987 Wh L^{-1}. Further improvements in energy density are possible by optimizing the fuel pellet configuration (density, geometry, particle size and distribution, etc.). Energy density greater than 2000 Wh L^{-1} should be possible in optimized MFCs discharged at low-power.

Acknowledgments

This material is based upon work supported by Honeywell International. Any opinions, findings and conclusions or recommendations expressed in this material are those of the authors and do not necessarily reflect the views of Honeywell International.

References

[1] J.A. Paradiso, T. Starner, IEEE Pervasive Computing 4 (1) (February 2005) 18–27.
[2] L. Zhu, K.Y. Lin, R.D. Morgan, V.V. Swaminathan, H.S. Kim, B. Gurau, D. Kim, B. Bae, R.I. Masel, M.A. Shannon, Journal of Power Sources 185 (2008) 1305–1310.
[3] V.C.Y. Kong, F.R. Foulkes, International Journal of Hydrogen Energy 24 (1999) 665–675.
[4] R. Wood, T. Rezachek, Electrical Power Generator, US Pat. 7,001,681, Feb. 21, 2006.
[5] T. Rezachek, R. Wood, Electrical Power Generator, US Pat. 7,445,860, Nov. 4, 2008.
[6] S. Moghaddam, E. Pengwang, K.Y. Lin, R.I. Masel, M.A. Shannon, Journal of Microelectromechanical Systems 17 (2008) 1388–1395.
[7] S. Moghaddam, E. Pengwang, R.I. Masel, M.A. Shannon, Journal of Power Sources 185 (2008) 445–450.
[8] S. Eickhoff, R. Wood, Water Reclamation in a Micropower Generator, US Pat. 7901816, March 8, 2011.
[9] Steven Eickhoff, AMPGen Quarterly Status Report. DARPA MTO MEMS PI Meeting (December 2004).
[10] L. Zhu, V. Swaminathan, B. Gurau, R.I. Masel, M.A. Shannon, Journal of Power Sources 192 (2009) 556–561.
[11] J. Kim, J. Lee, K. Choi, H. Chang, Journal of Power Sources 185 (2008) 881–885.